Anal. Bioanal. Electrochem., Vol. 12, No. 5, 2020, 663-687

Analytical& Bioanalytical Electrochemistry

2020 by CEE
www.abechem.com

Full Paper

A Novel Choline Biosensor Based on Immobilization of Enzyme Choline Oxidase on the β-Ga_2O_3 Nanowires Modified Working Electrode

Vahid Ghafouri ,* and Aghdas Banaei

Nano and Biophysics Department, Institution Research of Applied Sciences, Academic Center of Education, Culture and Research (ACECR), Shahid Beheshti University, P. O. Box 19615-1171 Tehran, Iran

*Corresponding Author, Tel.: +982122431933

E-Mail: vahid.ghafouri@ut.ac.ir ; vahid.ghafouri5@gmail.com

Received: 27 April 2020 / Received in revised form: 15 May 2020 / Accepted: 17 May 2020 / Published online: 31 May 2020

Abstract- This article is a report on a novel and high-stability biosensor with minor interference effects of surface modification of working electrode with β-Ga_2O_3 nanowires (NWs) on choline oxidase biosensor were investigated in an electrochemical detection system. β-Ga_2O_3 NWs were materialized on the silicon substrate in a catalyst-free growth mechanism. The β-Ga_2O_3 NWs were in string form with 10 µm in length and uniformly 30 nm in diameter. Then the enzyme choline oxidase (ChOx) immobilized on the β-Ga_2O_3 NW/CB arrays on the working electrode. The Cyclic voltammetry (CV), Impedance spectroscopy and differential pulse voltammetry (DPV) measurements were performed for bio-sensing detection with choline chloride as substrate. One of the most prominent features of this surface modification with Ga_2O_3 NWs /CB is that the peak intensity, which is often of the order of µA, is greatly increased and reaches about mA. Chronoamperometry amplification well confirms the performance of this surface modification. The current with the CB modified electrode is about three times more than the non-modified electrode, and Ga_2O_3 NWs/CB modified electrode twice more than the CB modified electrode. The maximum current in the DPV data is modelled linearity i_{ap}= 0.159 (C)+2.28 and R^2 = 0.982. The limit of detection (LOD) of the electrode for the choline measurement was reached to 8.29 µM. The Sensitivity of the electrode was around 0.0397 mA mM^{-1} mm^{-2}. The stability of this biosensor has been well studied over a period of 6 months, and more than 80% of the permanency of its response has been confirmed.

Keywords-Ga_2O_3 Nanowires; Electrochemical biosensor; choline oxidase; screen-printed electrode; amperometry

1. INTRODUCTION

Electrochemical procedures supply a hopeful approach to decrease the response time and have less interference from turbidity [1,2]. Additionally, electrochemistry also has the advantages of prolonged lifetime, high accuracy, low detection limit and good reproducibility [3]. Electrochemical sensors have been used for many analyses, such as in clinical [4], biological [5], environmental [6], and pharmaceutical [7]. The attraction of applying electrochemical sensors based on their high sensitivity, cheap, appropriate selectivity, and the facility of action, prompt analytical time, and easy pretreatment procedure. Electrochemical sensors include biosensors such as enzyme electrode [8], ion-selective electrodes [9] and metal electrodes [10]. The determination of analyte has been accomplished by voltammetry with carbon paste electrodes [11], glassy carbon electrodes [12], and amperometric procedures are also reported [13]. Lately, many researchers are focusing on ameliorate the analytical performance of electrochemical sensors [14]. Highly sensitivity is one of the main keys to obtain more precise detection results. Exploiting nanomaterials to electrochemical sensors have found able to enhance the effective surface area of electrodes and accelerate electron transfer across the electrode surface, thus improve the sensitivity and the stability of analytical response [6, 15]. The performance of biosensors is influenced by the physical and chemical properties of the materials used in their building.

Compared to 2D thin films where binding to the surface leads to redox reaction on the surface of a planar device such as working electrode of three –electrode electrochemical cell, oxidation and reduction in the 1D nanostructure takes place in the “boundary” of the 1D nanostructure thus giving rise to large changes in the electrical properties that potentially enables the detection of a single molecule. Thus 1D nanostructures avoid the reduction in signal intensities that are inherent in 2D thin films as a result lateral current shunting. This property of the 1D nanostructures provides a sensing amplification for label-free and direct electrical readout when the nanostructure is exploited as electrode material on an electrochemical cell. Such label free and direct detection is particularly desirable for rapid and real-time monitoring of receptor–ligand interaction with a receptor-modified nanostructure, particularly when the receptor is a biomolecule such as antibody, DNA, and Enzyme. Additionally, the sizes of biological macromolecules, such as proteins and nucleic acids are comparable to nanoscale building blocks. Hence, any interaction between such molecules should induce significant variations in the electrical properties of 1D nanostructures. Further, 1D nanostructures offer new capabilities not available in larger scale devices [16].

Choline, a vital nutrient that plays a key role in physiological processes, it is especially important and undoubtedly is one of the most important substances in the body's metabolism [17]. Choline can be found in several different arenas as a substantial segment in many plants and animal organs, e.g. bile, brain, egg yolks, hops, belladonna, as an essential nutrient in

human breast milk, or as a constituent of different biological fluids, e.g. amniotic liquid and blood. Choline is an effective and leading precursor of acetylcholine, a neurotransmitter that is effective in maintaining memory and controlling muscles. [18]. Phosphatidylcholine (PC) is a major component of cellular plasma membrane [19]. Choline helps keep cell membranes functioning properly, prevents the build-up of homocysteine in blood (elevated levels are linked to heart disease), reduces chronic inflammation and plays a role in nerve communications. In pregnancy, Choline plays an equally important role to help prevent certain birth defects, such as spina bifida and brain development issues. Choline defect can affect memory and quickly cause liver dysfunction or cancer. Abnormal choline metabolism has been signified in a number of neurodegenerative disorders such as Alzheimer's and Parkinson's diseases [20].The signs of choline deficiency are fatty liver and hemorrhagic kidney necrosis. Free radical activity in livers with choline deficiency may be associated to the carcinogenesis method. Therefore, measuring and quantifying it is particularly important in the diagnosis of brain disorders such as Alzheimer's disease and Parkinson's. [21].

Enzyme-based choline biosensors have emerged in the recent years as the most promising method. The investigation on ChOx is of interest to scientists for a variety of reasons. Initial reports of the presence of choline oxidase in animal tissues were presented by Bernheim [22]. ChOx was first extracted from rat liver in 1938 [23]. ChOx from the soil bacterium Arthrobacter globiformis was purified and characterized by Ikuta et al. in 1977 [24]. An important barrier to the development of biosensors for in situ measurement is the high levels of selectivity required due to the complexity of the physiological environment. Enzyme-based biosensors offer selectivity via indirect recognition of the products of a specific enzymatic reaction. Amperometric enzyme microsensors suitable for in situ measurement of choline have been developed that utilize ChOx [25], and several have been tested in rat brains [26].

The development of biosensors for detection of choline, choline derivatives and organophosphorous compounds in biological [27] and environmental samples (including air, soil and water) [28] render this enzyme of clinical and industrial interest. Different configurations have been used for choline biosensors including redox intermediates, conductive polymers, carbon nanotubes, graphene, nanoparticles and their hybrid compounds [29-34].

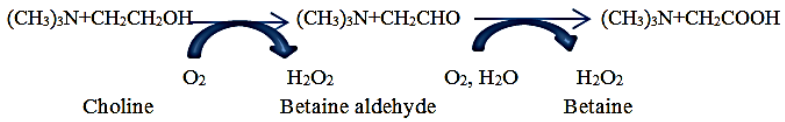

Scheme 1. Reaction catalysed by choline oxidase

Choline is converted by ChOx in the presence of oxygen, generating H_2O_2. Electroactive hydrogen peroxide can be consequently identified with various modified sensors or

electrodes (Scheme 1). Hydrogen peroxide (H_2O_2) as a by-product of the ChOx catalyst reaction plays a major role in amprometric-based measurements. In order to increase the H_2O_2 signal it reacts directly with the redox mediator [29, 30], or its reaction is catalyzed by a second enzyme [32].

One-dimensional (1-D) nanostructures have attracted significant research attention in a few years ahead due to their inimitable structural, electronic, optical, and mechanical properties and have been extensively studied due to their potentials as the building blocks for fabricating nanometer-scaled electronic, optoelectronic, electrochemical, and sensor devices. Semiconducting oxides, as an important series of materials candidates for sensors and biosensors, have attracted considerable attention in scientific research and technological applications. Various semiconducting nanowires, nanorods, and nanotubes of single element, oxide, and compound semiconductors have been successfully synthesized [35–38].

Recently, quasi-one-dimensional nanostructures for the functional materials have been successfully fabricated using various approaches including thermal evaporation [39-42], sol-gel [43], arc discharge [44], and laser ablation [45]. β-Ga_2O_3 is an attracting outstanding research interest as a potential candidate in several fields consisting solar-cell energy conversion, transparent conducting oxide (TCO), ultraviolet (UV) limiters ,flat-panel display, gas sensors and as anti-reflectance coatings [46, 47]. In the last decades, one-dimensional (1D) β-Ga_2O_3 structures including nanowires (MWs), nanorods, nanoribbones and nanobelts, more attention has been paid of researchers due to their excellent properties as compared to their bulk form. A significant supremacy of β-Ga_2O_3 NWs is their large surface to volume ratio supplying more surface states to interact with the adjacency. A number of utilizations have been evaluated for such 1D structures, including nanoscale devices [48] and sensor applications [49]. Newly, several reports have emerged on synthesis methods for crystalline gallium oxide nanostructures, for example, thermal evaporation, laser ablation, carbon thermal reduction arc-discharge, and metal-organic chemical vapor deposition [50].

To improve the electroanalytical performance of screen-printed devices, the inks can be modified during or after manufacturing with nanomaterials, such as metal nanoparticles (Au, Pt, Ag, etc.), carbonaceous nanomaterials (graphene, carbon nanotubes, carbon black, etc.), or conductive polymers (polypyrrole, polyaniline polythiophene, etc.). The use of nanomodified inks allows an enhancement of conductivity, defective sites, and high surface-to-volume ratio, boosting the analytical properties of the sensors [51, 52]. Among carbonaceous nanomaterials, carbon black (CB) has attracted considerable attention in the scientific community thanks to its outstanding properties in the electrochemical detection of several analysts. Furthermore, it is an inexpensive material that is easily dispersible in inks and solutions to modify the electrodes, and does not require any prior treatment before use [53].

In addition, the electrochemical study has revealed the best electrochemical behavior using printed electrodes modified by drop casting, probably ascribed to a higher content of

CB on the working electrode surface [54]. The printed electrodes modified with CB by drop casting approach have demonstrated their suitability as cost-effective and miniaturized electrochemical sensors for several analytics—including polyphenols, thiols, and phosphate—to name a few [55,56].

The aim of this work was present and comprehensive research on a novel electrochemical biosensor for the quantitative detection of ChOx using modified electrodes. For this purpose, a comprehensive investigation of choline oxidation at the enzyme-modified electrode was carried out by amperometric and impedimetric methods at different applied potentials. In this research, we used β-Ga_2O_3 NWs/ CB modified electrode as working electrodes for ChOx detection. Measuring the charge transfer resistance of a redox probe at the electrode interface is the basis of the work of Faradic based impedimetric systems. The impedance detection is sensitive, fast and with a low detection limit. The β-Ga_2O_3 NWs were grown in our laboratory by a vapor transfer method. Different electrode architectures were investigated by fixed potential amperometry and EIS for choline determination. This study presents the first impedimetric electrochemical detection of choline with Ga_2O_3 NWs modified electrodes and shows good response.

2. EXPERIMENTAL

2.1. Materials

Choline oxidase (EC 1.1.3.17 from Alcaligenes species), with an activity of 15 units/mg solid, choline chloride as substrate were supplied by Sigma (St. Louis, MO, USA). Potassium phosphate (K_2HPO_4 and KH_2PO_4) was purchased from Merck (Darmstat, Germany). Ga_2O_3 powder (99.999%, ~50–70 µm grain size) and graphite powder, Carbon Black (99.99%, ~70 µm) and Dimethylformamide (DMF) were supplied by Sigma. All electrochemical measurements were carried out at room temperature in a conventional screen-printed electrodes (SPEs) were purchased from Italsence (Electrode System: CE + RE+ WE, WE Material: Carbon, CE Material: Carbon, RE Material: Silver, Support Material: Polyester). All solutions were prepared with 0.05 M phosphate buffer, pH 7.4.

2.2. Growth of β-Ga_2O_3 nanowires

β-Ga_2O_3 NWs developed by Ga_2O_3 powder and graphite powder in 1: 1 ratio was mixed to form a homogenous source weighing 400 mg. For fabricating a choline biosensor, we have initially grown an array of Ga_2O_3 NWs on Si (100) via thermal evaporation, without using any catalyst. A high temperature furnace was used to grow β-Ga_2O_3 NWs. Freshly prepared Ga_2O_3 source powder and substrates were loaded in alumina boats in the high-temperature and low-temperature zones of the vacuum furnace. The furnace was initially evacuated to a pressure of 10-3 Torr and argon gas was then passed at a constant flow rate of 100 sccm. The

temperature of the furnace was approximately raised to 900–950 ^{o}C. The substrates were unloaded after the furnace was cooled to room temperature.

2.3. Modification of the Screen-Printed Electrodes and immobilization of ChOx on modified electrodes

A scheme of ChOx biosensor with modified Ga_2O_3 NWs /CB electrode was indicated in Fig. 1. SPEs consisted of a working electrode in carbon modified with Ga_2O_3 NWs /CB, a reference electrode in silver/silver chloride, and a counter electrode in carbon (Fig. 2). Printed electrodes were modified by drop casting as well as adding β-Ga_2O_3 NWs /CB powder in the DMF, reaching an improvement in terms of reduction of peak-to-peak separation and an increase of peak current intensity as electrochemical probe .

The casting solution was obtained by mixing 5 µL of 0.1 M DMF in 10 mM ethanol on the surface of the working electrode. The drop was carefully pipetted to be localized exclusively on the working electrode area. Then, 5 µL of this solution was drawn by micropipette and carefully inserted on the surface of the working electrode. The solution was left on the electrode for 10 min and then rinsed with a few mL of 10 mM ethanol. The electrodes were then left 60 min in the oven at 40 °C. The Ga_2O_3 NWs/CB modified electrodes were stored dry at room temperature in the dark.

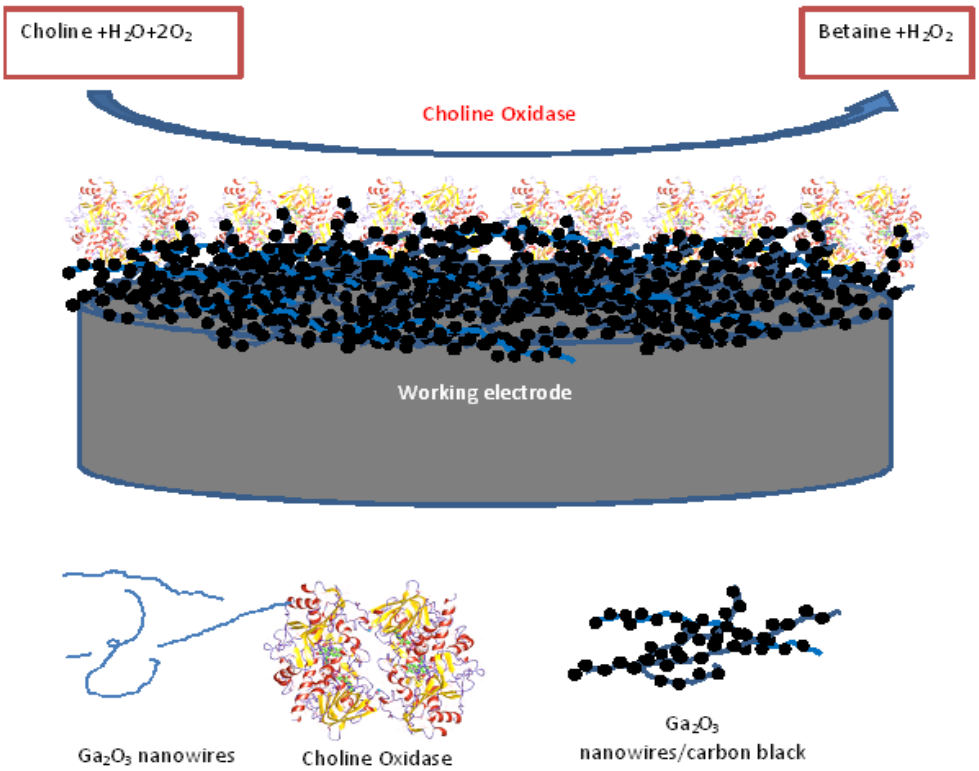

Fig. 1. A scheme of ChOx biosensor with modified Ga_2O_3 NWs /CB electrode

After thought the ChOx was immobilized on Ga_2O_3 NWs array. 10 µL ChOx (2.9 mg /mL ChOx dissolved in 0.05 M phosphate buffer pH 7.4) was dropped onto the nanowire surface and enzyme was immobilized on it via physical adsorption. The newly constructed electrode was allowed to dry over 2 hours at room temperature prior to use.

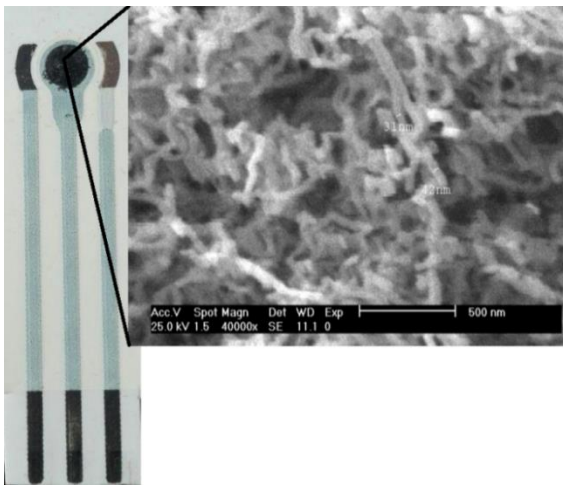

Fig. 2. Photo of an SPE modified with Ga_2O_3 NWs /CB. Inset: SEM image of the working electrode modified with Ga_2O_3 NWs /CB (Ga_2O_3 NWs /CB diameter 90 ± 10 nm)

2.4. Electrochemical measurements

For the amperometric choline detection, phosphate buffer electrolyte solutions (PBSs 0.05 M) with pH 7.4 were prepared from standard stock solutions of KH_2PO_4 and K_2HPO_4. All solutions were prepared with deionized water. Choline chloride was dissolved in PBS and kept at 4°C. We used 1-10 mM choline chloride (choline chloride dissolved in buffer solution) as substrate for ChOx enzyme for all of the electrochemical experiments .

All measurements were carried out using three-electrode screen printed system. This system uses carbon as counter electrode (CE), Ag/AgCl as reference electrode (RE), and Ga_2O_3 NWs /CB modified electrode as working electrode (WE). Electrochemical measurements were carried out using a portable potentiostat EmStat3 (Palmsens, The Netherlands) and the fitting of the data was obtained by using Z-view software (PSTrace 5).

The measurements were performed using cyclic voltammetry (CV), Impedance spectroscopy and differential pulse voltammetry (DPV). Functional conditions for electrochemical measurements were summarized in Table 1. For the better performance of the electrodes, the electrode pretreatment process was performed using a phosphate buffer at cyclic voltammetry in the range of potential between -1 V and +1 V with a scan rate of 100 mVs^{-1} for 20 cycles. The impedance spectra were recorded in the frequency range 0.005 Hz to 5 kHz at the redox equilibrium potential. Voltammetric measurements were taken using a 0.05 M PBS under quiescent condition and scan rate of 100 mVs^{-1}. Stock solutions were

made by dissolving phosphate buffer electrolyte and choline chloride solutions. Concentrations of choline chloride /PBS used to obtain the calibration curve were 1-8 mM. Limit of detection (LOD) and sensitivity of ChOx were determined from the calibration curve. The calibration curve was plotted from the anodic peak current at the maximum potential.

Table 1. Functional conditions for electrochemical measurements

Impedance spectroscopy	Scan type: Fixed Potential E_{dc} = 0.8 V E_{ac} = 0.1 V Frequency type: scan Max frequency = 5 kHz Min frequency = 0.005 Hz
Cyclic Voltametry	E_{begin} = 0.0 V $E_{vertex1}$ = -1.0 V $E_{vertex2}$ = +1.0 V E_{step} = 0.01 V Scan rate = 100 mV/s
Chronoamperometry	E_{dc} = -0.3 V, +0.2V $t_{interval}$ =6 s t_{run} = 180 s
Differential Pulse Voltametry	E_{begin} = -1.0 V E_{end} =1.0 V E_{step} =0.5 V Scan rate =100 mV/s

2.5. Characterization

As synthesized products were characterized by X-ray diffraction with Cu-Kα radiation (Philips X'pert Pro diffractometer), field emission scanning electron microscopy (FE-SEM, Hitachi S-800), and transmission electron microscopy (Philips, CM-30). TEM specimens were prepared by ultrasonicating the Ga_2O_3 NWs in methanol and dispersing a drop of solution on a carbon-coated copper grid.

3. RESULTS AND DISCUSSION

3.1. Ga_2O_3 nanowires morphology

Fig. 3 shows the very long, stranded nanowires with a length of more than 10 micrometers and a uniform NW diameter of about 30 nm. These NWs have a proper bonding and cover the surface completely homogeneously and uniformly. The aspect ratio (length to diameter ratio) of these NWs is about 300. Due to the morphological characteristics of these NWs, the use of these NWs will be very powerful in sensing applications. Because the surface-to-volume ratio of these NWs is very high, it causes the receiver or electron donor reactor to react well to its electrical connections

and increases the electron exchange between the interconnecting phase and the reactant. This will be due to the electrochemical reactions of creating an inner Helmholtz plane between the NWs and the electrolyte solution (diffuse layer).

The Inset image shows the TEM image of NWs, in which case the NWs up to less than 10 nm in diameter can be easily observed. Fig. 4 (a) shows the XRD pattern of β-Ga_2O_3 NWs for the sample that it located at the distance of 16 cm from evaporation source. All relatively sharp diffraction peaks can be perfectly indexed to β-Ga_2O_3 with a monoclinic structure, which is in good agreement with the reported values of β-Ga_2O_3 with the lattice constants a = 12.24 Å b = 3.04 Å, c = 5.81 Å, β = 103.76°. Fig. 4 (b) indicates the results of EDS analysis. As it can be seen, only C, O and Ga elements present in EDS analysis results. It confirms that the β-Ga_2O_3 NWs /carbon black composite established on the modified working electrode.

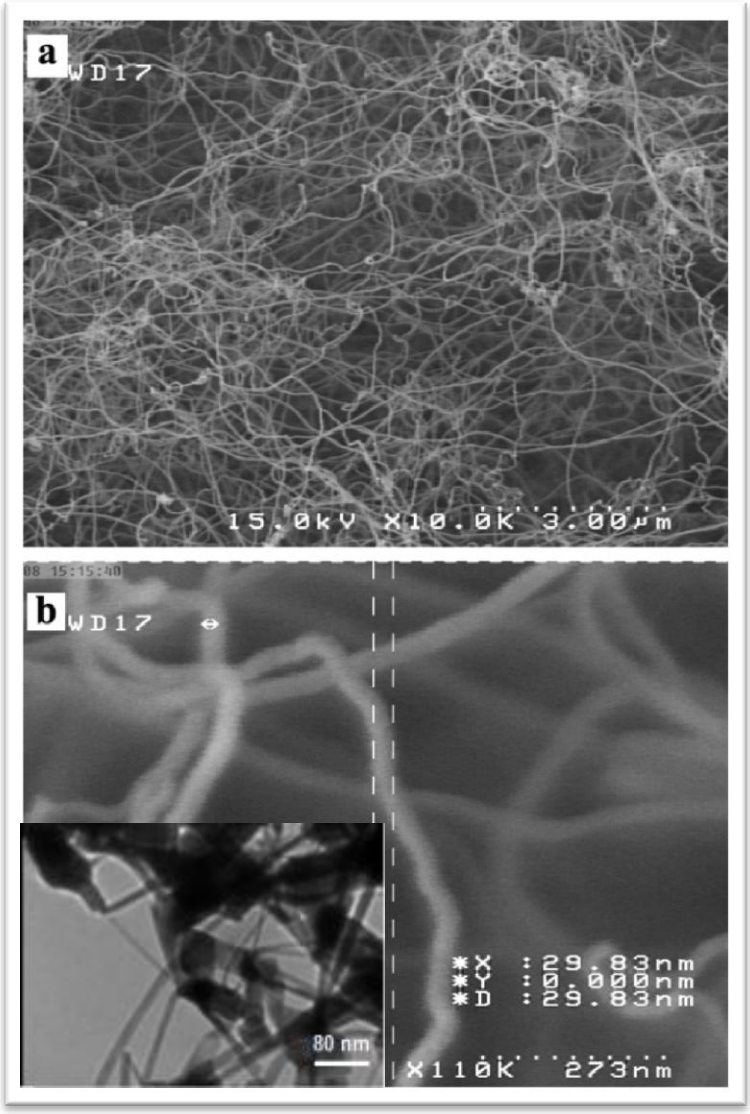

Fig. 3. Nanowires with a length of more than 10 micrometers and a uniform NW diameter of about 30 nm. The aspect ratio of these NWs is very high (about 300). Inset the TEM image of NWs less than 10 nm in diameter

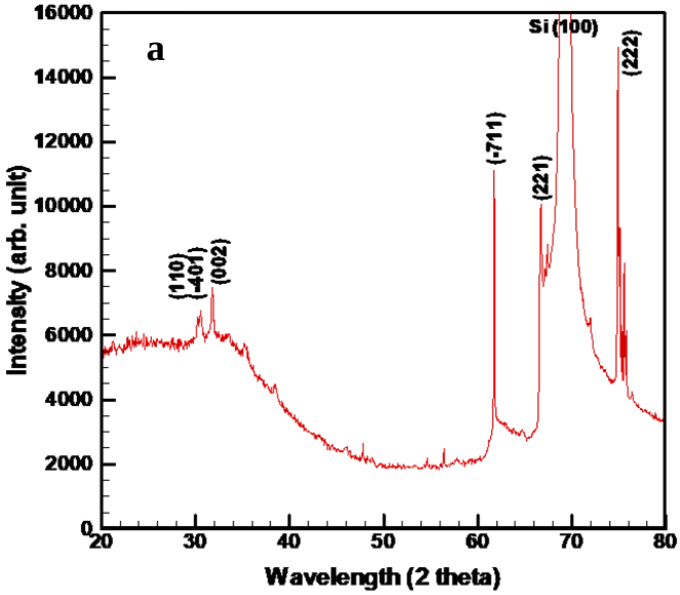

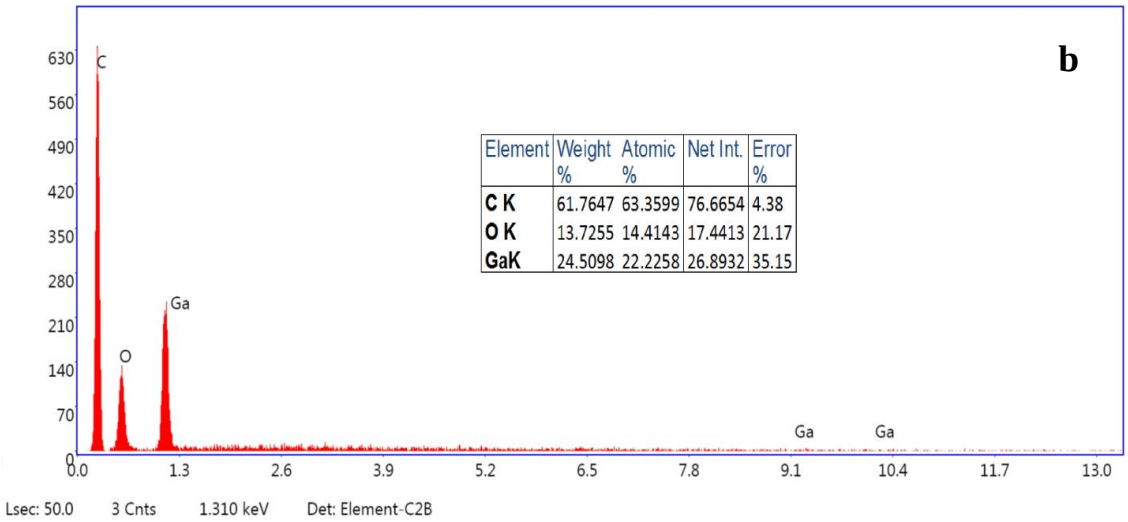

Fig. 4. (a) XRD pattern of β-Ga_2O_3 NWs at the distance of 16 cm from evaporation source. **(b)** EDS analysis for β-Ga_2O_3 NWs-carbon black nanocomposite

3.2. Effect of pH

As stated by the prior report [57], we expect that the redox response of choline chloride would be associated to pH, and among other buffers, we chose the PBS buffer. In order to determine this, the differential pulse voltammetry of choline chloride was obtained in 0.50 mM concentration of choline chloride solutions with varying pH from 5.8 to 8.0 Fig. 5 (a) at a surface of β-Ga_2O_3-CB/ carbon electrode. It can be seen that maximum value of the peak current was emerged at pH 7.4 Fig. 5 (b), so the optimum amount was observed at pH 7.4.

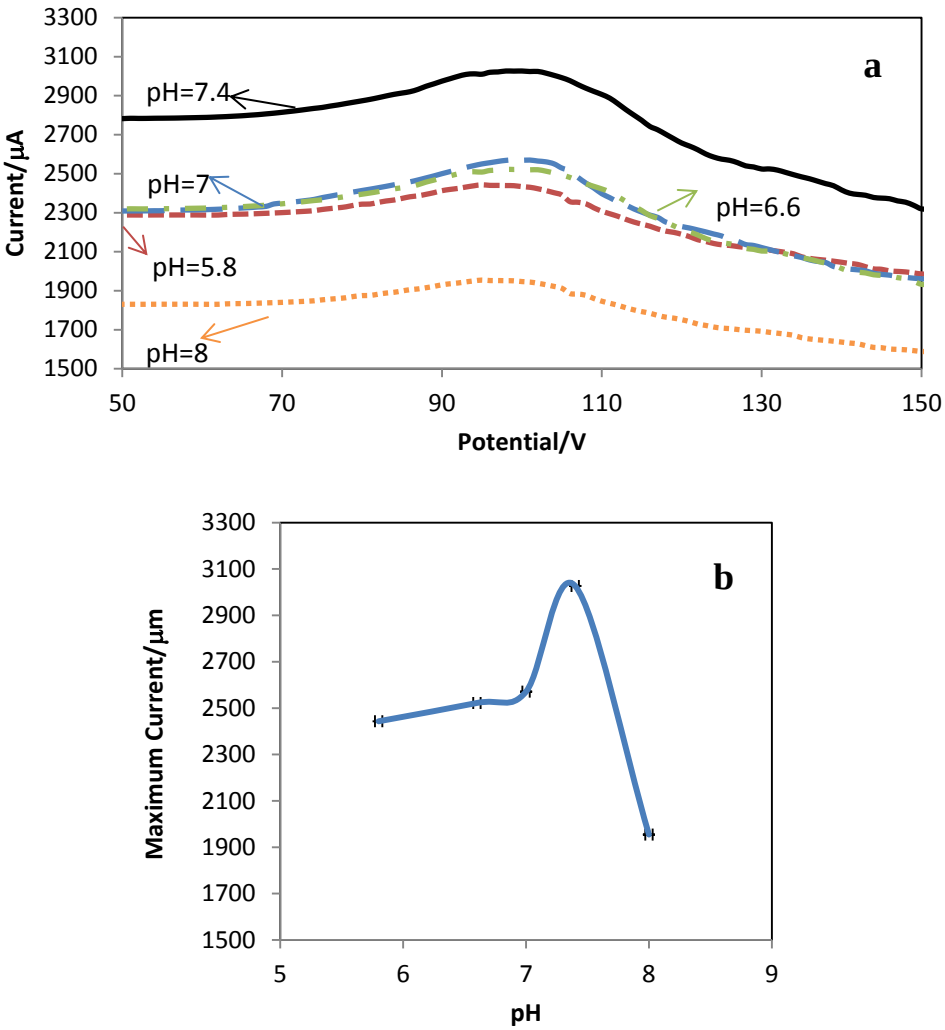

Fig. 5. (a) Influence of pH on differential pulse voltammetry of choline chloride at a surface of the modified electrode, (pH 5.8, 6.6, 7, 7.4, and 8, respectively). **(b)** Current-pH curve for electro oxidation of 5 mM choline chloride at surface of β-Ga_2O_3-CB/ carbon electrode with a scan rate of 100 mV s^{-1}

3.3. Electrochemical measurement of Ga_2O_3 NWs /CB modified electrodes in presence of ChOx enzyme and choline chloride as substrate

Data obtained from electrochemical measurement was used to analyze the performance of Ga_2O_3 NWs /CB on the ChOx enzyme and choline chloride as substrate. Fig. 6(a) shows the cyclic voltammogram for three different states without using substrate. The dot diagram shows a case where the working electrode was not modified with any surface modification and only ChOx was immobilized on the working electrode. From this diagram it is obvious that the redox peaks are very weak and no significant signal change in the CV diagram is evident. The dashed line graph shows a case where the working electrode was first modified with CB and then ChOx was immobilized on it. As can be seen with this modification, tangible changes occur in the CV cycle, and especially in the oxidation branch. The oxidation

peak in this case shows about 0.12 mA, which was not previously visible. The solid line shows the working electrode modified with a mixture of Ga_2O_3 NWs /CB powder and then ChOx was immobilized on it. In this graph, the oxidation and reduction peaks increase dramatically, and the effect of this surface modification of the working electrode can be clearly seen in the redox signals amplification. In the oxidation branch, the current is approximately three times that of the previous state, which the surface is modified with CB, and at the reduction branch the peak has reached at 0.52 mA. As we could see from Fig. 6(a) the cathodic and anodic current increase with modification of working electrode with Ga_2O_3 NWs /CB.

Fig. 6(b) shows the CV diagram with different concentrations of choline chloride from 0 to 9 mM.

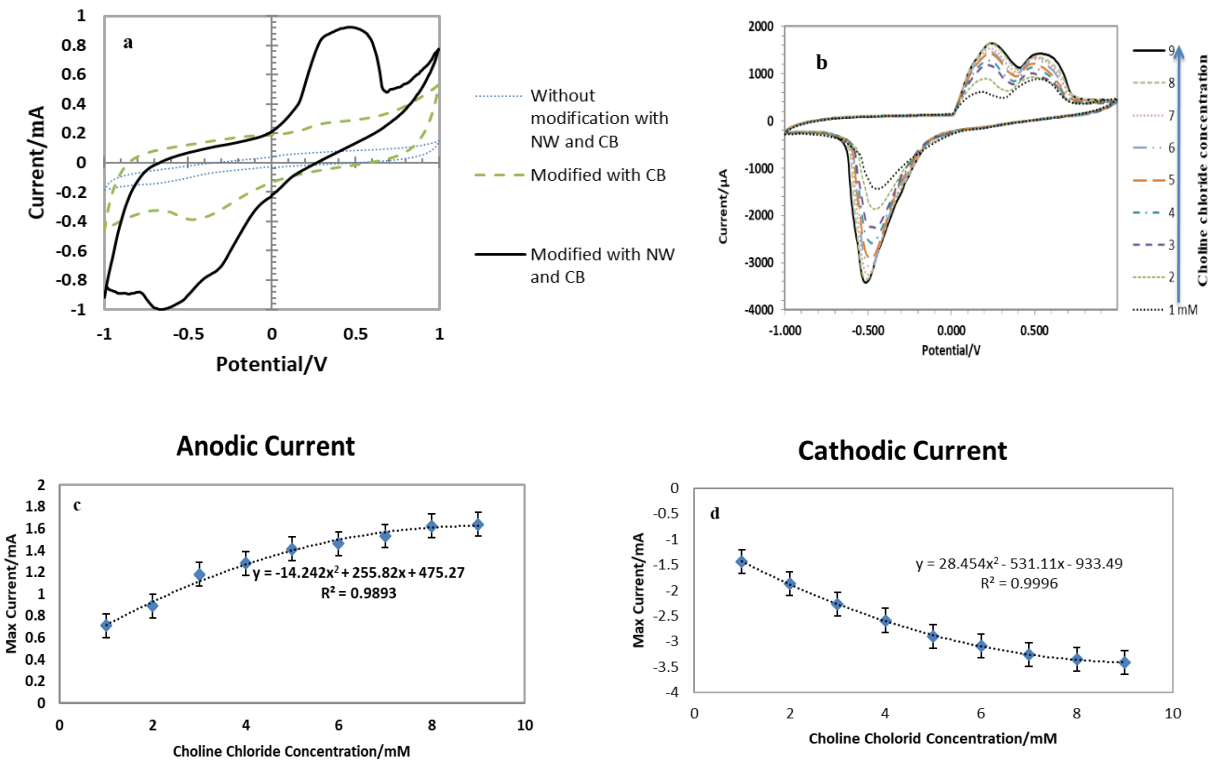

Fig. 6. (a) Cyclic voltammogram for three different states. The dot diagram with any surface modification and only the working electrode was immobilized with the ChOx. The dashed line graph shows a case where the working electrode was first modified with CB powder and then immobilized with ChOx. The solid line shows the working electrode modified with a mixture of Ga_2O_3 NWs /CB powder. **(b)** The CV diagram with different concentrations of choline chloride analyte from 0 to 9 mM. Amplification of redox sites induced by ChOx enzyme with choline chloride substrate has been well demonstrated. **(c)** and **(d)** The linearity limit and parabolic behaviour of the reinforcement of anodic and cathodic currents for different concentrations of choline chloride.

Amplification of redox sites induced by ChOx enzyme with choline chloride substrate has been well demonstrated. By adding the choline chloride, the CV diagram in the anodic branch has a double peak and its CV behaviour changed to an acceptable state. What is well observed is that as the concentration of choline chloride increases, the intensity of oxidation peaks decreases to less than 6 mM, which is parabolic at concentration above 6 mM, indicating saturation of the concentration of choline chloride. One of the most prominent features of this surface modification with Ga_2O_3 NWs /CB is that the peak intensity, which is often of the order of µA, is greatly increased and reaches about mA. This feature makes it possible to best demonstrate the properties of ChOx biosensor using this surface modification, and it is competitive with commercially available biosensors.

The upward trend of the reduction and oxidation peak currents in the CV diagram is shown in diagrams Fig. 6(c) and (d), respectively. The trend of increasing peak currents for the oxidation branch and decreasing incremental behaviour are regular. At first, as the concentration of choline chloride increases, a linear incremental behaviour is observed, which behaves to a certain extent, and then the behaviour becomes parabolic, indicating a saturation state. As can be seen, at concentrations of 1 to 9 mM, the maximum cathode current behaviour is determined by a coefficient of determination R^2 equal to 0.989 and at concentrations of 1 to 9 mM, the minimum anodic current behaviour is equal to 0.999, they are well parabolic order 2.

Chronoamperometry is a very useful potential-step voltammetry method. An applied electrode potential at the electrode surface forces the electron mediator reaching the electrode surface immediately undergoing an electron transfer reaction. Fig. 7 illustrates the chronoamperometry response for ChOx biosensor by modifying working electrode with Ga_2O_3 NWs /CB. Fig. 7(a) indicates a comparison between the three different biosensor performance modes in the presence of different working electrode surface modifications. For these curves Edc = -0.3 V. In the dotted graph, the response of the chronoamperomety is in the state where the working electrode is unmodified with NWs and CB and only ChOx was immobilized on it. The dashed line diagram shows this response when the working electrode surface was first modified with CB and then ChOx was immobilized on it. And the solid line diagram shows the working electrode modified with a mixture of NWs and CB and then ChOx was immobilized on it. Chronoamperogram current amplification well confirms the performance of this surface modification.

In the chronoamperograms, capacitive behavior is important. In the case of the working electrode corrected with carbon black because the capacitance does not change dramatically, the final current approaches zero. The capacitance was increased when working electrode was pre- modified with CB and then ChOx was immobilized on it. The presence of Stern layer and Helmholtz plans increase the charge of the double layer and increase the current.

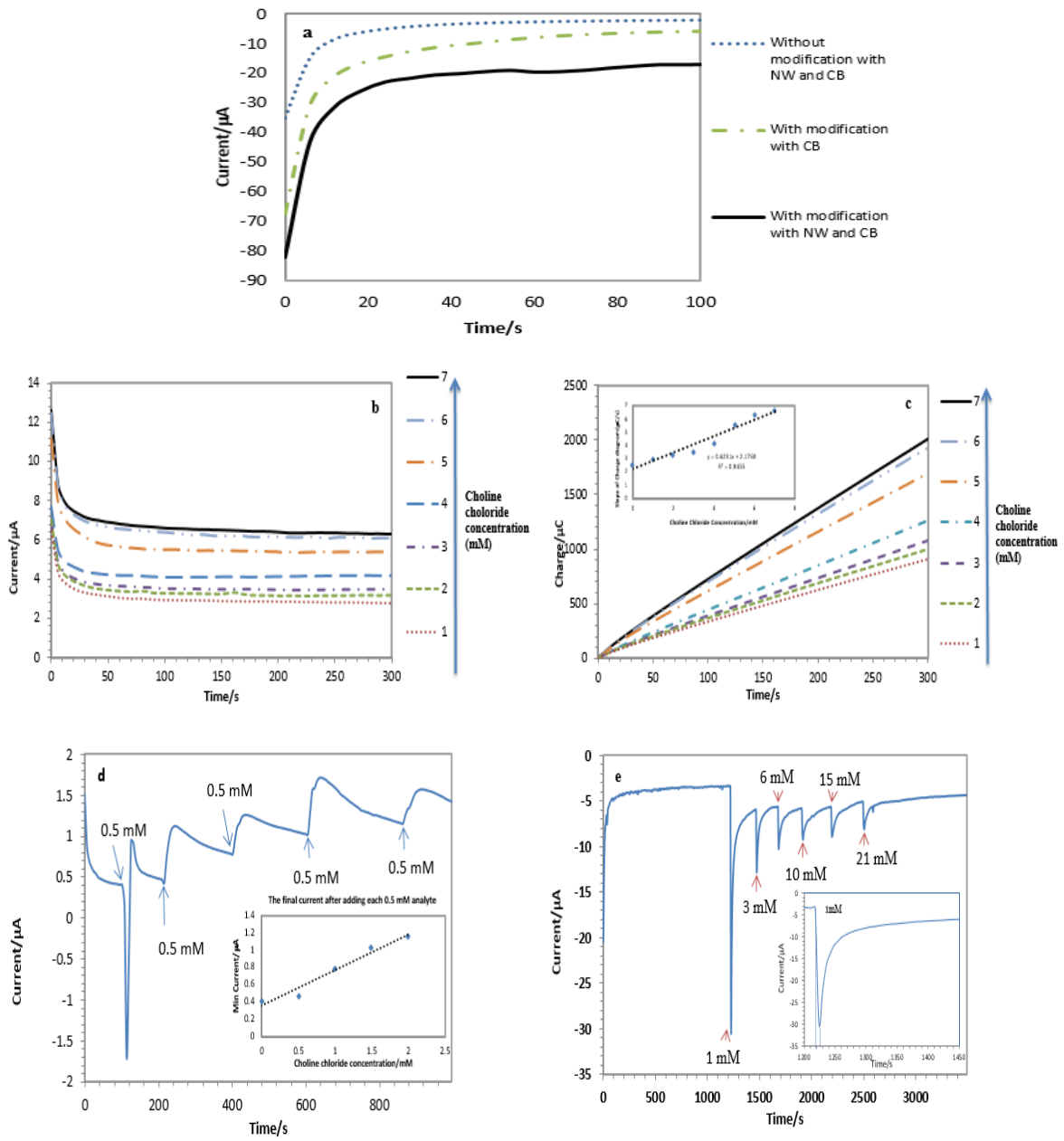

Fig. 7. The chronoamperograms for ChOx biosensor by modifying working electrode with Ga_2O_3 NWs /CB. **(a)** A comparison between the three different modes of biosensor performance in the presence of different surface modifications of the working electrode, E_{dc}=-0.3V. **(b)** The chronoamperograms for different choline chloride concentrations, E_{dc}=+0.2V. **(c)** The changes of the electric charge are plotted over time and for different choline chloride concentration. The inset graph is the electric charge slope in terms of concentration, which proves its linearity. **(d)** The instantaneous response of the ChOx biosensor to a Ga_2O_3 NWs modified electrode. The inset graph is the minimum current after reaching the steady state of biosensor response. **(e)** The rapid response to the addition of choline chloride analytes. The inset graph indicates the fast response and return to the minimum current after adding the analyte. Response time is about 10 s.

In the third case, when the NWs were mixed with CB and the working electrode was modified with them, and then ChOx was immobilized on it, there is an increase in the surface-to-volume ratio at the electrode surface such as paralleling a large number of capacitors, which leads to a significant increase in capacitance capacity and ultimately to an increase the saturated current.

Fig. 7(b) shows the chronoamprograms for different amounts of choline chloride. As the concentration of choline chloride increases, the current of the biosensor with respect to the time is amplified and the current increases. The uniform and constant current response indicates the stability and uniformity of biosensor performance over time. When the choline chloride analyte is added to the electrolyte, it initially acts as an H^+ ionic booster, reducing surface resistance and greatly enhancing the current. After increasing the concentration of choline chloride, this agent acts as an insulator and reduces the saturation current.

In Fig. 7(c) the changes of the electric charge are plotted over time and for different amounts of choline chloride concentration. As can be seen, while the concentration of choline chloride increases, the charge behavior increases linearly with time. The internal shape of the electric charge slope is plotted in terms of concentration, which proves its linearity.

Fig. 7(d) shows the instantaneous response of the ChOx biosensor with a Ga_2O_3 NWs /CB modified electrode. In this diagram, for relatively low values of analyte concentration at specified time intervals and then steady state current has been studied. By adding the biosensor analyte it responds instantly and the electrical current in the diffusion layer changes and a good quality response is provided. Over time, the current decreases and returns to steady state, but it will increase slightly due to the additional loads caused by the analyte flow. The rapid response to the addition of choline chloride analyte is shown in Fig. 7(e). In the first step, after the addition of choline chloride to the electrolyte, a significant increase in current is observed. After the state reaches the saturation point it is amplified by adding more analyte but does not reach the initial current. For a closer look, we should increase the concentration of analyte each time to see a clear response to the increase in choline chloride concentration. The response time is about 10 s.

3.4. Long-term storage stability

Electrodes were dipped in a phosphate buffer solution (pH 7.4, 0.05 mM) and kept at 4°C in a refrigerator.CV diagram for choline chloride of with different concentration was tested every 30 days, up to 6 month. The response current even now preserved above 80% of the primary activity, which must be associate with the high relative surface area of the β-Ga_2O_3-CB/ carbon electrode, increasing the adsorbability between enzyme and electrode, and also diminishing enzyme dropping. Fig. 8 indicate the CV diagrams (a) 90 days after the modification and (b) 180 days after the modification.

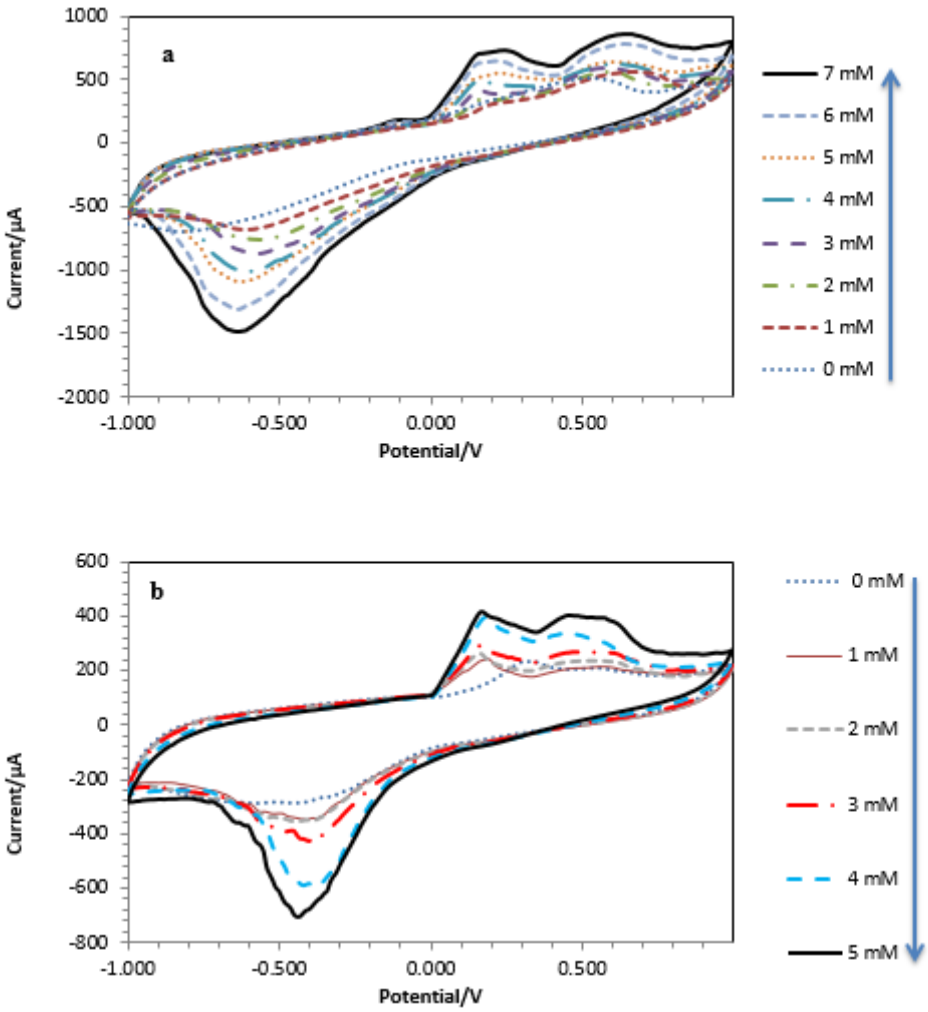

Fig. 8. Response of long term storage stability of biosensor on the CV diagram for different concentrations of choline chloride analyte **(a)** After 90 days **(b)** After 180 days

3.5. Impedance spectroscopy (EIS) study

A comparison of the performance of Ga_2O_3 NWs /CB modified electrode and unmodified electrode with enzyme ChOx immobilization was also studied using electrochemical impedance spectroscopy (EIS). In Fig. 9 the electrochemical impedance behavior of the ChOx biosensor is evaluated using choline chloride substrate and by surface modification of the working electrode with Ga_2O_3 NWs /CB. It was discovered that there was a significant difference between the electrodes without and with modification measurement. Fig. 9(a) shows the response of the imaginary part of the admittance in terms of its real part. As can be seen, the surface modification of the working electrode has led to a significant increase in the admittance response, indicating the optimization of the biosensor performance and its improved performance in the presence of Ga_2O_3 NWs /CB. This also can be seen that Ga_2O_3 NWs /CB capacitance after ChOx measurement is higher than the initial value before

measurement. This is because the ChOx enzyme oxidation product attaches on the surface of the Ga_2O_3 NWs /CB modified electrode.

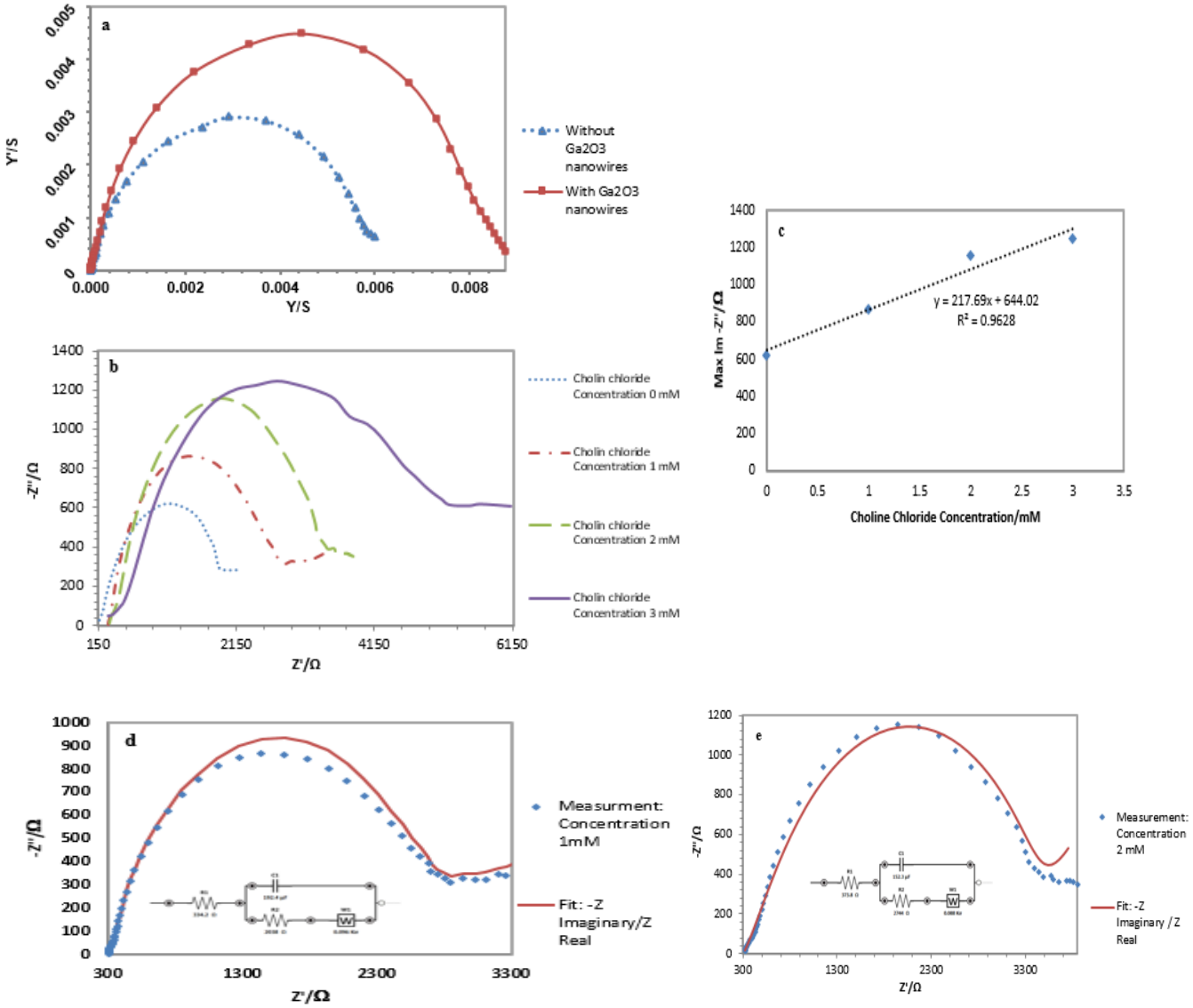

Fig. 9. The electrochemical impedance behavior of the ChOx/Ga_2O_3 NWs /CB biosensor using choline chloride substrate. **(a)** The response of the imaginary part of the admittance versus its real part. **(b)** the Nyquist plots of biosensor for different choline chloride concentrations. **(c)** the maximum of imagnary part of impedance vesuse cholin chloride concentration. **(d)** and **(e)** The equivalent impedance response circuit of this biosensor is equated and plotted for the two concentrations of 1 and 2 mM with the corresponding measurement Nyquist plots, respectively.

This pattern is attributed from the nanostructured surface or rough electrode surface, which contributes to the rise of the constant phase element in the high frequency region. This

occurrence can be explained by the pseudo capacitance that associated with the surface-bound functional groups [58, 59].

Fig. 9(b) shows the Nyquist plots are designed for different amounts of choline chloride concentration for the biosensor with a modified working electrode. What is observed is that at low and high frequencies there is a proportional response for different concentrations of choline chloride and its linear performance is acceptable. Its linear function is shown in Fig. 9 (c).

The equivalent impedance response circuit of this biosensor for two concentrations of 1 and 2mM is plotted with the corresponding Nyquist plots in Fig. 9(d) and (e), respectively. Capacitive behavior and how the Warburg impedance form and function both substantially and efficiently validate impedance responses.

Impedance parameters, i.e. R_1 (solution resistance), R_2 (charge transfer resistance) and C constant phase element were simulated using an equivalent circuit, which are shown in Fig. (d) and (e). Using the equivalent circuit in Fig. 9(d), we can write the following equations. Capacitance (C) as a function of frequency can be evaluated using the following equation [60].

$$Z_c = -j/C\omega \tag{1}$$

$$Z_w = \frac{\sigma(1-j)}{\sqrt{\omega}} \tag{2}$$

where ω is the angular frequency and Z_w impedance of Warburg element .

$$Z = Z' + R_1 \tag{3}$$

$$Z' = \frac{(R_2+Z_w)Z_c}{Z_c+Z_w+R_2} \tag{4}$$

as a result

$$Z_R = R_1 + \frac{a+b}{C\omega[(a+b)^2+(1+b)^2]}$$

$$Z_I = -\frac{(a+b)^2+b(1+b)}{C\omega[(a+b)^2+(1+b)^2]} \tag{5}$$

where

$$a = R_2 C\omega \quad , \quad b = \sigma C\sqrt{\omega}$$

Based on this model if the Warburg impedance is eliminated, the equation is simplified as follows:

$$\mathrm{Z_R} = \mathrm{R_1} + \mathrm{R_2}/(1 + \mathrm{R_2^2}\omega^2\mathrm{C}^2) \tag{6}$$

$$\mathrm{Z_I} = -\mathrm{R_2^2}\omega\mathrm{C}/(1 + \mathrm{R_2^2}\omega^2\mathrm{C}^2) \tag{7}$$

In the high frequency range ($\omega >> 1$) the impedance is equivalent to the solute resistance (R_1) and in the low frequency range ($\omega \rightarrow 0$) the impedance is equivalent to the total solubility and charge transfer resistance ($R_1 + R_2$).

Betaeine was the oxidizing product from ChOx. The possible mechanism of ChOx reversible reaction and the interaction between the Ga_2O_3 NWs /CB modified electrodes with ChOx are presented in Fig. 10. Hydrogen bond acceptor count for Ga_2O_3 is equal to 3 and hydrogen bond donor count for choline is equal to 1. There are three types of O sites in β-Ga_2O_3 cell as shown in Fig. 10. As a result, three O vacancies exist, which are denoted as V_{OI}, V_{OII} and V_{OIII}, respectively. For V_{OI}, there are two 6-fold Ga ions and one 4-fold Ga ion surrounded, while two 4-fold Ga ions and one 6-fold Ga ion are adjacent to V_{OII}. The free electrons from the oxygen atoms of hydroxyl groups on ChOx temporarily bond to the electrode. This in turn causes the oxygen atoms to become unstable and hence releasing hydrogen atoms, thus forming an oxidation product (ChOx enzyme).

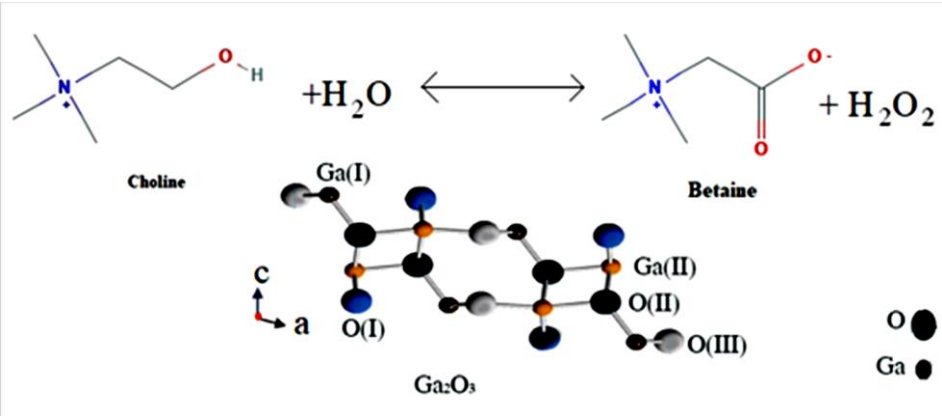

Fig. 10. The possible mechanism of reversible reaction of ChOx and the interaction between the Ga_2O_3 NWs /CB modified electrodes with enzyme

The effective cross-sectional area of the modified electrode increases due to enhancement of the surface-to-volume ratio in Ga_2O_3 NWs and considering the interaction between the stern layer, which occurs between redox in the ChOx enzyme and the working electrode surface, the amount of positive and negative ions has increased in this modified electrode and leads to increase conductivity and ultimately increase the electrical conductivity and current, and decrease the apparent resistance.

3.6. Calibration curve of ChOx / Ga_2O_3 NWs /CB electrodes

Calibration curve was obtained from electrochemical measurements using various concentrations of choline chloride as a substrate for ChOx. The measurement was conducted using DPV with potential sweep of -1.0 V to 1.0 V and scan rate of 100 mV/s. The choline chloride voltammograms at various concentrations are shown on Fig. 11(a). The anodic

current increased as choline chloride concentration increases. Fig. 11(b) indicate the concentration versus peak of anodic current (i_{pa}) at DVP diagram, in which we used to obtain calibration curve with maximum current in DPV in various concentrations of choline chloride (0-8 mM) and at pH 7.4. Scan rate is 100 mV/s. The maximum current in the DPV data is modeled linearity as i_{ap} = 0.159 (C) + 2.28 and R^2 = 0.982.

This calibration curve was used to determine the LOD and the sensitivity of the Ga_2O_3 NWs /CB modified electrode on the choline chloride solution. The LOD of the biosensor was found at 8.29 μM. The sensitivity of the electrode was calculated from the linear regression equation in Fig. 11(b), which was 0.0397 mA mM^{-1} mm^{-2}. The observed sensitivity is much higher than previously reported ChOx sensors. A comparison of the analytical performances of some ChOx biosensors fabricated based on different materials and modifications of electrode surfaces for electrochemical approaches are listed in Table 2.

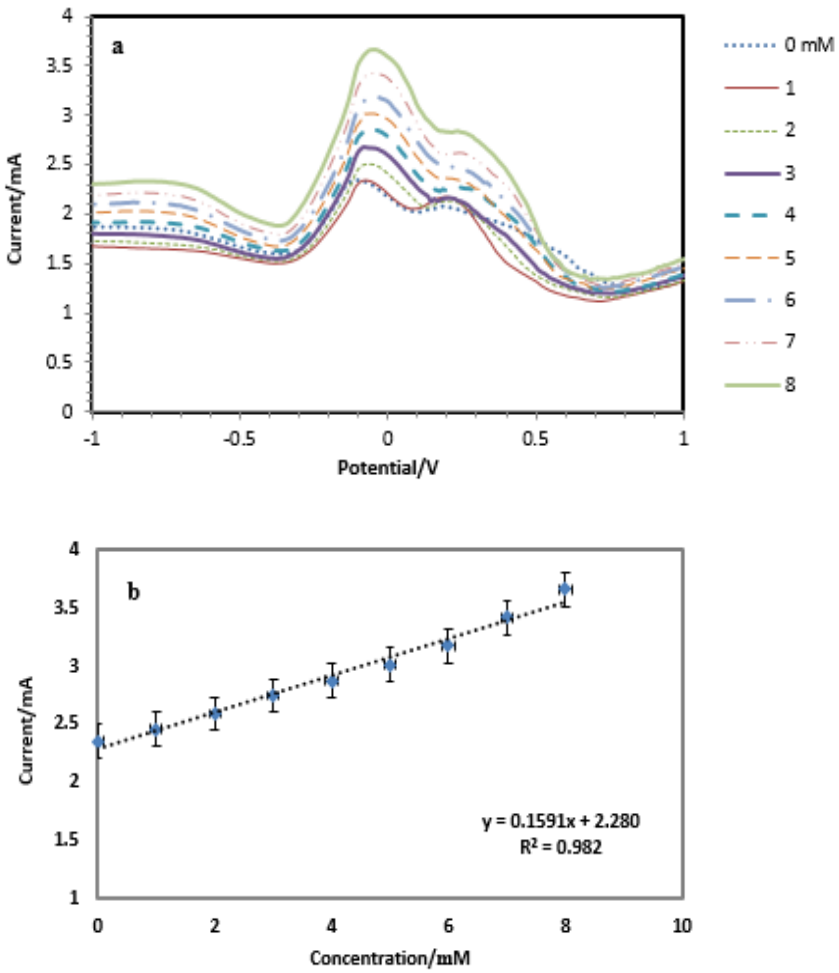

Fig. 11. (a) Differential Pulse Voltammograms of ChOx/Ga_2O_3 NWs /CB modified electrodes for various concentration of choline chloride (1-8 μM). Scan rate is 100 mV/s. **(b)** Maximum current in DPV versus various concentration of choline chloride. Scan rate is100 mV/s.

Table 2. Comparison of the analytical performances of some ChOx biosensors fabricated on different materials and modifications of electrode surfaces for electrochemical approaches

Materials/methods	LOD	Sensitivity	Response time	Linearity, r^2	Ref.
Multienzymes-ChOx/ pmPD/Pt/CV	0.33 ± 0.09 mM	-	< 1s	0.997	[61]
ChOx/polyacrylamide microgels/Etd	8.0 mM	1.745 mA M^{-1} cm^{-2}	-	0.9944	[62]
Fe_3O_4 magnetic NPs/SWV	0.1 nM	-	-	0.995	[63]
Gold screen-printed/silica biocomposites	6.0 mM	6.0 mA mM^{-1}	-	-	[64]
Ch-ChOx/TGA-SAM/chip/CV	0.012 nM	3.5 mA mM^{-1} cm^{-2}	~10 s	0.9938	[65]
ChOx/Ga_2O_3 NW/CB/Carbon screen-printed	8.29 µM	0.0397 mA mM^{-1} mm^{-2}	~ 10s	0.982	Current work

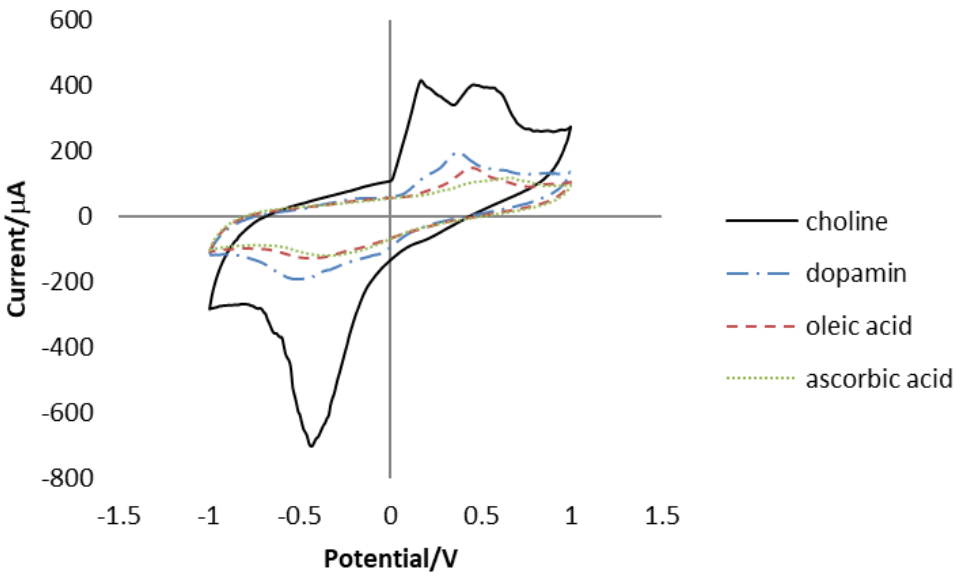

Fig. 12. The CV diagram with different kind of interfering species in comparison to the choline chloride analyte

3.7. Interference effects

The effects of three kinds of interfering species (dopamine, oleic acid and ascorbic acid) on CV response of the biosensor were investigated. Interfering species with concentration 5 mM in the biosensor response for choline with 5 mM concentration is shown in Fig. 12. Although anodic and cathodic peaks are seen in the CV diagrams for these interfering species, but they CV responses are very small in comparison to the CV response of choline. So, as interfering species they have little effect on biosensor response. However, further studies on the intervening species in this biosensor are needed, and we are examining other interfering species and their effects on this biosensor.

4. CONCLUSION

In this paper we introduce a novel and high sensitive electrochemical biosensor with high-stability and minor interference effects. Choline is a vital nutrient that plays a key role in physiological processes, and it is an important and undoubtedly one of the most important substances in the body's metabolism. Modification of β-Ga_2O_3 NWs /CB electrode as working electrodes for choline detection was performed, and a comprehensive investigation of choline at the enzyme-modified electrode was conducted by amperometric and impedimetric methods at different applied potentials. Ga_2O_3 NWs /CB modified electrode has been shown a good performance as an electrochemical biosensor for choline detection. The measurements using CV, EIS and DPV indicated that the different electrode characteristics before and after choline measurements. The maximum current in the DPV data is modelled linearity and the limit of detection (LOD) of the electrode for the choline measurement was acceptable in the range of biosensors. The stability of this biosensor has been well studied over a period of 6 months, and it has been confirmed that more than 80% of the response permanency.

Acknowledgements

The authors would like to thank Academic Center of Education, Culture and Research (ACECR) for support.We have also to express our appreciation to the Dr. Mohsen Shariati for sharing their pearls of wisdom with us during this research.

REFERENCES

[1] J. Mohanraj, D. Durgalakshmi, R. Ajay Rakkesh, S. Balakumar, S. Rajendran, and H. Karimi-Maleh, J. Coll. Int. Sci. 566 (2020) 463.

[2] H. Karimi-Maleh, C. T. Fakude, N. Mabuba, G. M. Peleyeju, and O. A. Arotiba, J. Coll. Int. Sci. 554 (2019) 603.

[3] A. Khodadadi, E. Faghih-Mirzaei, H. Karimi-Maleh, A. Abbaspourrad, S. Agarwal, and V. K. Gupta, Sens. Actuators: B. Chemical 284 (2019) 568.
[4] C. I. Justino, T. A. Rocha-Santos, and A. C. Duarte, TrAC Trends Anal. Chem. 45 (2013) 24.
[5] P. Bollella, G. Fusco, C. Tortolini, G. Sanzo, G. Favero, L. Gorton, and R. Antiochia, Biosens. Bioelectron. 89 (2017) 152.
[6] N. L. W. Septiani, B. Yuliarto, and H. K. Dipojono, Appl. Phys. A. 123 (2017) 166.
[7] Y. Song, Y. Luo, C. Zhu, H. Li, D. Du, and Y. Lin, Biosens. Bioelectron. 76 (2016) 195.
[8] C. Menzel, T. Lerch, T. Scheper, and K. Schügerl, Anal. Chim. Acta, 317 (1995) 259.
[9] V. M. Shkinev, B. Y. Spivakov, G. A. Vorob'eva, and Y. A. Zolotov, Anal. Chim. Acta. 167 (1985) 145.
[10] Z. Chen, D. R. Marco, and P. W. Alexander, Anal. Commun. 34 (1997) 93.
[11] G. Lu, and X. Wu, Talanta 49 (1999) 511.
[12] T. Matsunaga, T. Suzuki, and R. Tomoda, Technol. 6 (1984) 355.
[13] S. M. Harden, and W. K. Nonidez, Anal. Chem. 56 (1984) 2218.
[14] M. Miraki, H. Karimi-Maleh, M. A. Taher, S. Cheraghi, F. Karimi, Sh. Agarwal, and V. K. Gupta, J. Mol. Liq. 278 (2019) 672.
[15] M. R. Shahmiria, A. Baharia, H. Karimi-Malehb, R. Hosseinzadeh, and N. Mirnia, Sens. Actuators B 177 (2013) 70.
[16] A. K. Wanekaya, W. Chen, N. V. Myung, and A. Mulchandani, Electroanalysis. 18 (2006) 533.
[17] J. J. Langer, M. Filipiak, J. Keci´nska, J. Jasnowska, J. Włodarczak, and B. Buładowski, Surf. Sci. 573 (2004) 140.
[18] T. Misgeld, R. W. Burgess, R. M. Lewis, J. M. Cunningham, J. W. Lichtman, and J. R. Sanes, Neuron 36 (2002) 635.
[19] S. S. Razola, S. Pochet, K. Grosfils, and J. M. Kauffmann, Biosens. Bioelectron. 18 (2003) 185.
[20] Z. Zhang, J. Wang, X. Wang, Y. Wang, and X. Yang, Talanta 82 (2010) 483.
[21] M. Sánchez-Paniagua López, J. P. Hervás Pérez, E. López-Cabarcos, and B. López-Ruiz, Electroanalysis 19 (2007) 370.
[22] F. Bernheim, and M. L. C. Bernheim, Am J. Physiol. 104 (1933) 438.
[23] P. J. G. Mann, H. E. Woodward, and J. H. Quastel, J. Biochem. 32 (1938) 1024.
[24] S. Ikuta, S. Imamura, H. Mistake, and Y. Horiuti, J. Biochem. 82 (1977) 157.
[25] M. G. Garguilo, N. Huynh, A. Proctor, and A. C. Michael, Anal. Chem. 65 (1993) 523.
[26] J. Cui, N. V. Kulagina, and A. C. Michael, J. Neurosci. Methods, 104 (2001) 183.
[27] H. Tavakoli, H. Ghourchian, A. A. Moosavi-Movahedi, and F. C. Chilaka, Int. J. Biol Macromol. 36 (2005) 318.

[28] A. Guerrieri, L. Monaci, M. Quinto, and F. Palmisano, Analyst. 127 (2002) 5.
[29] H. Zhang, Y. Yin, P. Wu, and C. Cai, Biosens. Bioelectron. 31 (2012) 244.
[30] A. H. Keihan, S. Sajjadi, N. Sheibani, and A. A. Moosavi-Movahedi, Sens. Actuators B-Chem. 204 (2014) 694.
[31] S. Sajjadi, H. Ghourchian, H. A. Rafiee-Pour, and P. Rahimi, J. Iran Chem. Soc. 9 (2012) 111.
[32] K. Deng, J. Zhou, and X. Li, Electrochim. Acta 95 (2013) 18.
[33] F. Qu, M. Yang, J. Jiang, G. Shen, and R. Yu, Anal. Biochem. 344 (2005) 108.
[34] S. Pundir, N. Chauhan, J. Narang, and C. S. Pundir, Anal. Biochem. 427 (2012) 26.
[35] Y. Xia, P. Yang, Y. Sun, Y. Wu, B. Mayers, B. Gates, Y. Yin, F. Kim, and H. Yan, Adv. Mater. 15 (2003) 353.
[36] J. H. Park, H. J. Choi, Y. J. Choi, S. H. Sohn, and J. G. Park, J. Mater. Chem. 14 (2004) 35.
[37] V. Ghafouri, A. Ebrahimzad, and M. Shariati, Scientia Iranica. 20 (2013) 1039.
[38] V. Ghafouri, M. Shariati, and A. Ebrahimzad, Scientia Iranica. 19 (2012) 934.
[39] Z. R. Dai, J. L. Gole, J. D. Stout, and Z. L. Wang, J. Phys. Chem. B 106 (2002) 1274.
[40] M. Shariati, and V. Ghafouri, Int. J. Modern Physics B. 28 (2014) 16 1450101.
[41] M. Shariati, and V. Ghafouri, The European Phys. J. Appl. Phys. 65 (2014) 20404.
[42] V. Ghafouri, M. Shariati, and A. Ebrahimzad, J. Nanoparticle Res. 16 (2014) 2309.
[43] F. Krumeich, H. J. Muhr, M. Niederberger, F. Bieri, B. Schnyder, and R. Nesper, J. Am. Chem. Soc. 121 (1999) 8324.
[44] Y. C. Choi, W. S. Kim, Y. S. Park, S. M. Lee, D. J. Bae, Y. H. Lee, G. S. Park, W. B. Choi, N. S. Lee, and J. M. Kim, AdV. Mater. 12 (2000) 746.
[45] Y. H. Tang, Y. F. Zheng, N. Wang, I. Bello, C. S. Lee, and S. T. Lee, Appl. Phys. Lett. 74 (1999) 3824.
[46] M. Ogita, K. Higo, Y. Nakanishi, and Y. Hatanaka, Appl. Surf. Sci. 175 (2001) 721.
[47] K. Shan, G. X. Liu, W. J. Lee, G. H. Lee, I. S. Kim, and B. C. Shin, J. Appl. Phys. 98 (2005) 023504.
[48] Y. Cui, Z. Zhong, D. Wang, W. U. Wang, and C. M. Lieber, Nano Lett. 3 (2003) 149.
[49] E. S. Snow, F. K. Perkins, and J. A. Robinson, Chem. Soc. Rev. 35 (2006) 790.
[50] K. W. Chang, and J. J. Wu, Adv. Mater. 17 (2005) 241.
[51] S. Cinti, and F. Arduini, Biosens. Bioelectron. 89 (2016) 107.
[52] F. Arduini, S. Cinti, V. Scognamiglio, D. Moscone, and G. Palleschi, Anal. Chim. Acta. 959 (2017) 15.
[53] S. Cinti, F. Arduini, M. Carbone, L. Sansone, I. Cacciotti, D. Moscone, and G. Palleschi, Electroanalysis 27 (2015) 2230.
[54] F. Arduini, F. D. Nardo, A. Amine, L. Micheli, G. Palleschi, and D. Moscone, Electroanalysis 24 (2012) 743.

[55] D. Talarico, F. Arduini, A. Constantino, M. D. Carlo, D. Compagnone, D. Moscone, and G. Palleschi, Electrochem. Commun. 60 (2015) 78.

[56] F. Arduini, M. Forchielli, A. Amine, D. Neagu, I. Cacciotti, F. Nanni, D. Moscone, and G. Palleschi, Microchim. Acta 182 (2015) 643.

[57] S. Zhao, Z. Zixia, Q. Xia, H. Jiadong, SH. Haibin, W. Baoyan, and CH. Qiang, Front. Chem. China. 2 (2007) 146.

[58] J. Kang, J. Wen, S. H. Jayaram, X. Wang, and S. K. Chen, J. Power Sources 234 (2013) 208.

[59] J. N. Barisci, G. G. Wallace, D. Chattopadhyay, F. Papadimitrakopoulos, and R. H. Baughman, J. Electrochem. Soc. 150 (2003) E409.

[60] J. Wang, Y. Xu, X. Chen, and X. Sun, Compos. Sci. Technol. 67 (2007) 2981.

[61] K. M. Mitchell, Anal. Chem. 76 (2004) 1098.

[62] M. S. P. Lopez, J. P. H. Perez, E. Lopez-Cabarcos, and B. Lopez-Ruiz, Electroanalysis 19 (2007) 370.

[63] Z. Zhang, X. Wang, and X. Yang, Analyst 136 (2011) 4960.

[64] I. Mazurenko, O. Tananaiko, O. Biloivan, M. Zhybak, I. Pelyak, V. Zaitsev, M. Etienne, and A. Walcarius, Electroanalysis 27 (2015) 1.

[65] M. M. Rahman, and A. M. Asir, Anal. Meth. 7 (2015) 9426.